Int J Adv Manuf Technol (2016) 87:2285–2292
DOI 10.1007/s00170-016-8593-5

ORIGINAL ARTICLE

Spindle axial thermal growth modeling and compensation on CNC turning machines

Kuo Liu[1] · **Yu Liu**[2] · **Mingjia Sun**[3] · **Xiaolei Li**[3] · **Yuliang Wu**[3]

Received: 15 October 2015 / Accepted: 2 March 2016 / Published online: 23 March 2016

Abstract Many studies indicate that thermal errors induced by spindle account for about 50–80 % of the total thermal errors of a machine tool due to the continuous rotation of the spindle during machining. The drawbacks of the commonly used axial thermal growth compensation methods for spindles were studied. In the present work, a robust axial thermal growth model for the spindle, based on the temperature variation, is proposed. Considering the exponential trend of the axial thermal growth of the spindle, the suggested model is based on an exponential formula. The results show that the steady value of axial thermal growth is changing with the spindle rotating speed. Therefore, the real-time steady value of axial thermal growth was predicted using the velocity and acceleration of temperature variation in the key point of the spindle. Additionally, the identification method for the parameters in the suggested model was also presented. The environmental temperature variation error (ETVE) and error induced by spindle rotation (EIBSR) were investigated using a CNC turning machine. The results recorded on the two turning machines indicated that high accuracy and strong robustness can be achieved with the suggested model, even when the rotating speed of the spindle changes randomly.

✉ Kuo Liu
liukuo0727@qq.com

[1] College of Mechanical Science and Engineering, Jilin University, Changchun 130025, China

[2] College of Mechanical Engineering and Automation, Northeastern University, Shenyang 110819, China

[3] State Key Laboratory, Shenyang Machine Tool (Group) CO., LTD, Shenyang 110142, China

Keywords CNC turning machine · Spindle · Thermal growth · Robustness

1 Introduction

The thermal error is a factor that significantly affects the accuracy stability of CNC machine tools. Many studies show that thermal errors account for 40–70 % of the total errors that may occur in machine tools [1, 2]. Thermal errors can mainly be minimized by two methods: error avoidance and error compensation. The error avoidance method strives to eliminate or reduce the thermal errors during the design or construction phase of machine tools [3, 4]. The error compensation method strives to create an opposite error that will eliminate the original thermal error. The error compensation method has many advantages, such as lower cost and a wide field of applications.

The total thermal errors in a machine tool include the spindle thermal error and the feed driving axes thermal errors [5]. The temperature fluctuation of the bearings, motors, and environment can cause spindle thermal errors, which are significant and cannot be ignored [6, 7]. Numerous experiments on turning machines and vertical machining centers indicate that spindle thermal errors account for approximately 50–80 % of the total thermal errors that can occur in a machine tool. As the spindle is always rotating during the machining process, but the movement range of the feed driving axis is narrow and its action intermittent. Various thermal error compensation methods have been widely studied, including the multiple regression method [8–11], neural network method [12–14], mechanism analysis method [15, 16], thermal mode method [17, 18], time series method [19, 20], and the support vector machine method [21–24].

Lei et al. [8] established a thermal error model based on the multi-variation autoregressive model for motorized spindles. The order and coefficient of the model are determined by using the Akaike information criterion and the least squares method, respectively. The results indicated that this model has improved accuracy than the temperature-based multiple linear regression models. Yang et al. [13] introduced an integrated recurrent neural network (IRNN) for spindle thermal errors. Xiang et al. [15] analyzed the spindle temperature field and thermal deformation and modified the preliminary theoretical model on the basis of thermal characteristics. The results showed that the new method is precise in predicting the spindle temperature field and thermal deformation during, both, the heating and cooling processes. Zhu [18] analyzed the thermal mode to determine the temperature key points and established a spindle thermal error model. Shu et al. [19] proposed the time series method for modeling micro-grinder thermal errors. Real-time excess temperature variables were used for the time series model, and the validity of the real-time excess temperature variables in the application of thermal error modeling, on the micro grinder, was proved. Lin et al. [21] established a thermal error model based on an adaptive, best-fitting, weighted least squares support vector machine. The parameters of weighted least squares support vector machine were optimized using a method called adaptive best-fitting parameter search algorithm. The samples were trained, and the weighted coefficients were calculated according to the error variables.

Although the aforementioned error modeling methods can be applied for error compensation, there are some drawbacks in these methods. These drawbacks include the following: (1) some methods only function under specific conditions, (2) more than one temperature sensors are required to achieve a high accuracy, which is relatively costly, and (3) these methods suffer from poor robustness. When the spindle rotating speed, during actual machining, is different from the thermal investigation, the predicted result becomes always poor, particularly for the multiple regression method. Continuing with the drawbacks, (4) long time is needed for thermal investigation, for instance, test data under various speeds is necessary in the time series method, in order to establish a good model, and (5) an artificial neural network can only be efficient when complete input and output information is used; mistakes may occur if inaccurate input and output information is used. Although the robustness of the mechanism analysis method is strong, the prediction for the temperature of the spindle, based on the heat-transfer mechanism, is hard to achieve.

It is clear that none of the aforementioned models is flawless; thus, an axial thermal growth model based on the temperature variation is proposed in the present study.

2 Spindle axial thermal growth model based on temperature variation

2.1 Modeling principle and derivation

Assuming that the wavy nature of the spindle axial thermal growth is exponential, the axial thermal growth error, E, increases exponentially before reaching the steady state thermal error E_{ss}, when the spindle rotates at the speed of n from the initial steady state condition (Fig. 1) [25].

During the transient process, the thermal growth, E, can be calculated according to Eq. (1).

$$E(i) = E(i-1) + (E_{ss}-E(i-1)) \times \left(1-e^{-\Delta t/\tau}\right) \tag{1}$$

where, $E(i)$ is the thermal growth at the time of i, $E(i-1)$ is the thermal growth at the time of $i-11$, Δt is the sampling period for thermal errors, τ is the mean time constant of the exponential curve.

The rotation speed is changeable in the actual machining process, which leads to the change of E_{ss} [25]. When the thermal growth does not continue following the previous exponential curve, due to the change in rotation speed, the temperature in the key point of the spindle will change correspondingly. Therefore, a temperature sensor should be set in the key point of the spindle. The change in rotation speed can be monitored using the changes in velocity and acceleration of the temperature. Furthermore, real-time steady value of the spindle thermal growth (E_{ss}) can be predicted using Eq. (2).

$$E_{ss}(i) = \alpha \times (T(i-1)-T(i-2)) + \beta \times \frac{\left(\left(T(i)-T(i-1)\right)-(T(i-1)-T(i-2))\right)}{\Delta t} \tag{2}$$

where, $E_{ss}(i)$ is the steady value of thermal growth at time i, $T(i)$ is the temperature in the key point of spindle at time i, α, and β are the response characteristic coefficients to be identified.

Figure 2 presents the spindle axial thermal growth model for different rotation speeds.

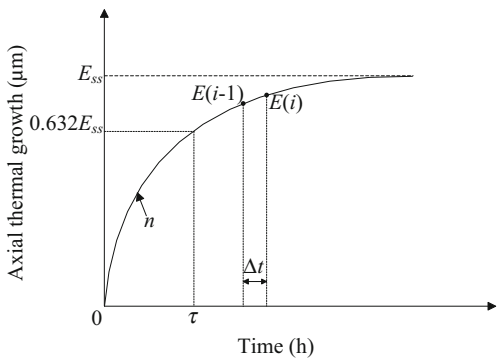

Fig. 1 Illustrative diagram of spindle axial thermal growth

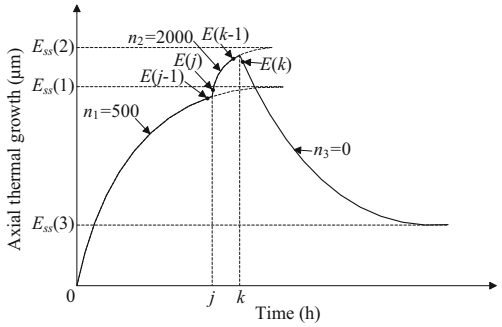

Fig. 2 Illustrative diagram of model at different rotation speeds

In Fig. 2, the thermal growth does not reach $E_{ss}(1)$, when time is $(j-1)$, during the rotation of the spindle at 500 rpm. Thereafter, the rotation speed of the spindle changes to 2000 rpm, when time is j, and $E(j)$ can be predicted according to Eq. (3).

$$E_{ss}(j) = \alpha \times (T(j-1)-T(j-2)) + \beta \times \frac{(T(j)-T(j-1))-(T(j-1)-T(j-2))}{\Delta t}$$
$$E(j) = E(j-1) + (E_{ss}(j)-E(j-1)) \times \left(1-e^{-\Delta t/\tau(2)}\right) \tag{3}$$

However, the thermal growth does not reach $E_{ss}(2)$, when time is $(k-1)$, and the rotation speed of the spindle changes to 0 rpm, when time is k. $E(k)$ can be predicted according to Eq. (4).

$$E_{ss}(k) = \alpha \times (T(k-1)-T(k-2)) + \beta \times \frac{(T(k)-T(k-1))-(T(k-1)-T(k-2))}{\Delta t}$$
$$E(k) = E(k-1) + \left((E_{ss}(k)-E(k-1)) \times \left(1-e^{-\Delta t/\tau(3)}\right)\right. \tag{4}$$

Since high frequency interference exists in the collected temperature data, the predicted value of thermal growth (E), calculated by the temperature, will contain high-frequency interference. Thus, filtering is essential to remove high-frequency interference in the compensation value. The filtering was performed using Eq. (5).

$$G(s) = \frac{E_f}{E} = \frac{a}{s+b} \tag{5}$$

where, E_f, is the compensation value after filtering and s is the Laplace operator.

Equation (5) can be changed to Eq. (6):

$$(s+b) \times E_f = a \times E \tag{6}$$

Furthermore, Eq. (6) can be changed to Eq. (7):

$$E_f(i) = -b \times E_f(i-1) + a \times E(i-1) \tag{7}$$

According to the analysis of the axial thermal growth model and based on temperature variation, it can be seen that the thermal growth can be predicted not only under constant rotation speed but also when changing the rotation speed. So, the robustness of the proposed model appears to be strong, regardless the spindle rotation speed.

2.2 Parameter identification

The parameters, such as α, β, and τ, need to be identified in Eqs. (1) and (2). The optimized values of α', β', and τ' can be obtained from Eq. (8).

$$\min\left[F\left(\alpha',\beta',\tau'\right)\right] = \sum_{m=1}^{M}\left(E_f(m)-E_t(m)\right)$$
$$\begin{array}{lllllll} lb & (1) & \le & \alpha & '\le & u & b \quad (1) \\ lb & (2) & \le & \beta & '\le & u & b \quad (2) \\ lb & (3) & \le & \tau & '\le & u & b \quad (3) \end{array} \tag{8}$$

where, E_t is the tested thermal growth.

The identification of α, β, and τ parameters in the thermal growth model is an optimization problem, including multiple variables and constraints. However, a penalty function needs to be established in the aforementioned optimization methods and the constraints can be eliminated in the optimization problem. However, this method has already been substituted by a new method based on the K-T equation, which is necessary for the optimization problem that needs constraints. Since quadratic programming problems needs to be solved in each calculation, this kind of method is termed as sequential quadratic programming method (SQP). The interior-point method was adopted as the optimization algorithm. It begins at an initial interior point in the feasible region and iterates sequentially the calculation of the minimum value.

The function "fmincon," which is provided in MATLAB software, employs the SQP method. So, "fmincon" function is used for the identification of parameters in thermal growth model. The call mode of "fmincon" is as follows:

```
[p, fval, exitflag, output] = fmincon (@opti1, xx0,
[],[],[],[], lb, ub, [], options);
Options = optimset ('Display', 'iter-detailed',
'Algorithm', 'interior-point', 'OutputFcn', @bansuifun,
'MaxFuneVals', …)
```

where *opti1* is the programming module for optimization and *optimset* is used for the set of the optimization options.

3 Experimental procedure

3.1 Experimental setup

The thermal growth of a spindle was tested on a CNC turning machine. The maximum rotational speed employed was 3000 rpm. Based on the correlation

analysis of error and temperature data, the temperature sensor was placed on the outer surface of the front bearing. The tested spindle and temperature sensor are presented in Fig. 3.

The thermal growth of the spindle was tested using the spindle error analyzer, manufactured by Lion Precision Corporation. It can test the spindle errors in three directions simultaneously. The sampling period for error data was set to 10 s, and the temperature data were collected using a temperature sensor. The sensor is developed independently, and the sensor chip is the Tsic506F (IST Corporation, Switzerland), with an accuracy of 0.1 °C (5–45 °C) and a resolution of 0.034 °C. Also, the shell material of the sensor is composed of magnets, which attracts ferrous materials. The experimental setup for measuring spindle axis thermal growth is presented in Fig. 4.

3.2 ETVE of the spindle

The variation of environmental temperature may lead to thermal errors of the spindle. In order to analyze the influence of the environmental temperature on the thermal growth of the spindle, ETVE was tested using the method described in [26]. The temperature and thermal growth of the spindle were tested for 24 h, at a speed of 0 rpm. The results are presented in Fig. 5.

The correlation coefficient of error was found to be −0.06, which reveals the irregularity of thermal growth of the spindle at a normal range temperature. This could be attributed to the joint interfaces of "inspection bar–spindle–bed–X axis–tool holder–frock–displacement sensor." The actual thermal expansion rate of each part is different, and the ETVE will be unequal to 0. However, the fluctuation range of ETVE was found to be −2 to 0 μm. Thus, it can be claimed that the influence of environmental temperature to the thermal growth is insignificant. However, if the tested ETVE was found to be higher, the thermal growth, induced by the spindle rotation, would need to be separated from the total thermal growth data.

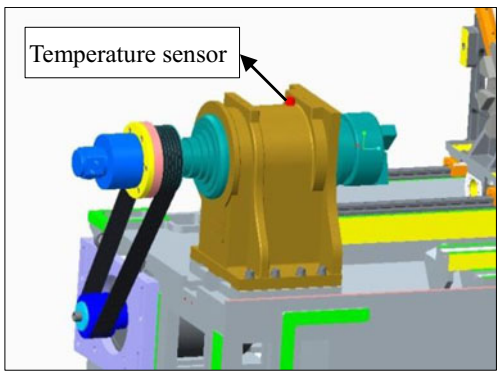

Fig. 3 Temperature sensor installation on the spindle

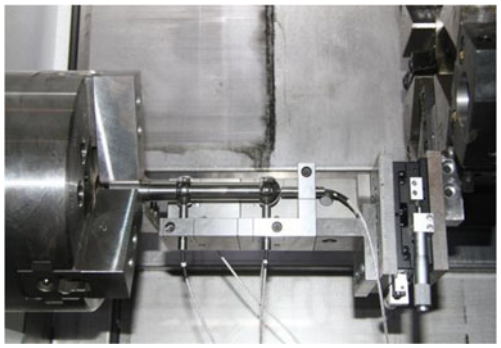

Fig. 4 Experimental setup for measuring spindle axis thermal growth

3.3 EIBSR of the spindle

Regarding the experiment mentioned in Section 3.2, the error induced by spindle rotation (EIBSR) will be studied in this section. The temperature and thermal growth were tested at a rotational speed of 500, 1000, 1500, or 2000 rpm. In each test, the spindle rotates at a preset rotating speed for 4 h and then remains stationary for 3 h. The results are presented in Figs. 6 and 7. It can be observed that the rise of temperature in the front bearing of the spindle is approximately 4–7 °C and the maximum value of the thermal growth 8–16 μm (Figs. 6 and 7). Also, the temperature and thermal growth increase when the rotating speed increases.

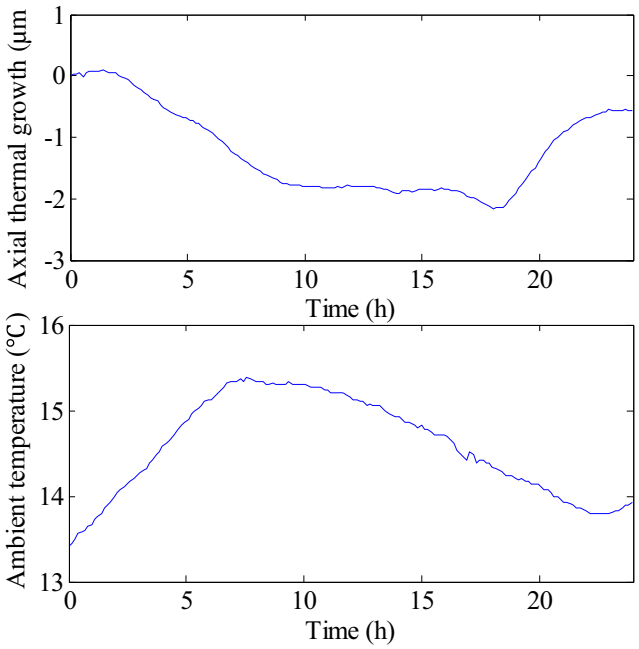

Fig. 5 Tested results of ETVE

4 Verification

4.1 Parameter identification

The parameters in the model will be identified based on the results in Section 3.3. The following equation (Eq. 9) was substituted into Eq. (1).

$$\gamma = 1 - e^{-\Delta t/\tau} \tag{9}$$

where, Δt is constant when the sampling time is determined. It can be observed that the time constant, τ, is constant during the warming up and cooling down phases at all speeds (Fig. 7). Thus, γ can be set as the same value for all speeds, in order to simplify the parameter identification process. Hence, Eq. (1) gives Eq. (10).

$$E(i) = E(i-1) + \gamma \times (E_{ss} - E(i-1)) \tag{10}$$

Consequently, the solution for α, β, and τ is changed to the solution for α, β, and γ.

4.2 Simulation verification

Simulation was carried out using the MATLAB R2014a software. The suggested temperature-based model (M I) was compared to the model (M II) in reference [25], which is based on the rotating speed to illustrate the advantages of the suggested model. The process for obtaining the parameters in M II was introduced in reference [25]. In Fig. 8, M I used the parameters identified at 1000 rpm. Table 1 clearly presents the residual errors of these two models for all speeds.

It is evident that the prediction accuracy of M Iwas higher than that of M II. Moreover, test data of the various speeds is essential for establishing the M II and long testing times are needed. Finally, even if the rotating speed of the spindle becomes different from that of the proposed model, the predicted results are still satisfactory.

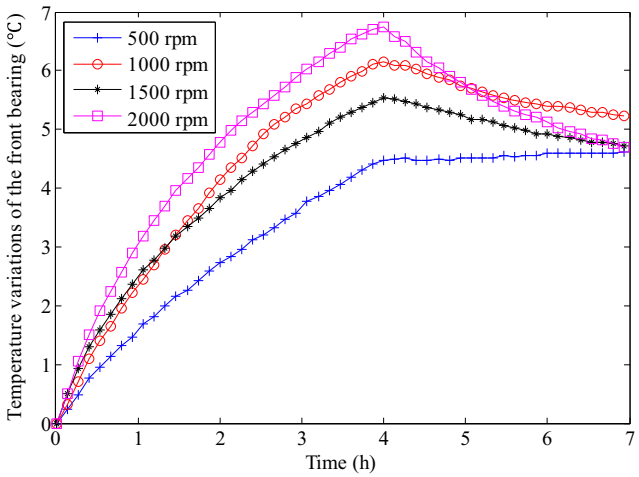

Fig. 6 Temperature variations for various rotating speeds

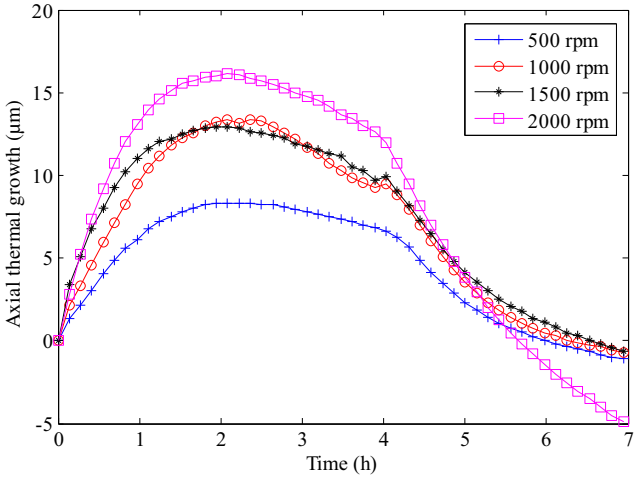

Fig. 7 Spindle axial thermal growth for various rotating speeds

4.3 Experiment verification

4.3.1 Communication configuration

In this section, the compensation effects will be verified using the spindle error analyzer. For this, the temperature data need to be collected and the compensation values need to be input to Z-axis of the turning machine in real-time. The external mechanical coordinate offset (EMCO) was used for writing the compensation values for FANUC 0*i*-TD CNC. The illustrative diagram of the compensation, based on EMCO, is presented in Fig. 9.

The communication between the thermal compensator and FANUC 0*i*-TD was achieved through Ethernet. The IP address of the thermal compensator and FANUC 0*i*-TD should be set in the same section. FANUC Open CNC API Specifications 2 (FOCAS2), which is provided by Fanuc Inc., was called in MATLAB. The main program segment for communication configuration is as follows:

```
loadlibrary ('Fwlib32.dll', 'fwlib32.h'); %Loading FOCAS2 library
sIPAddress = get (handles.cncaddress, 'String'); %Get IP of CNC
iPort = str2num (get (handles.com, 'String')); %Set port
lTime = 5; %Set sampling period
[Conection_Ret, IP, CNC_Handle] = calllib ('Fwlib32', 'cnc_allclibhndl3', sIPAddress, iPort, lTime, CNC_Handle); %Get the handle of FOCAS2 library
```

The writing of compensation values can be performed by using the function "pmc_wrpmcrng" regarding the communication configuration.

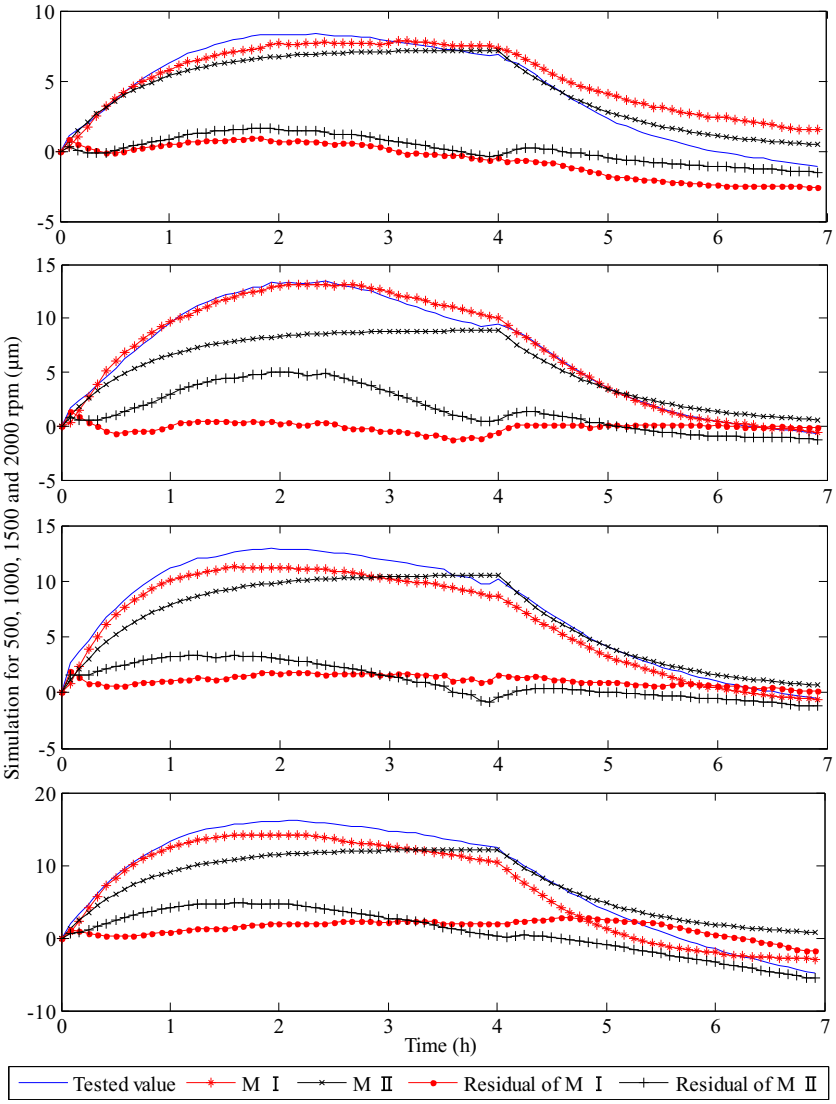

Fig. 8 Simulation results

4.3.2 Experimental results

Experimental verification was carried out based on the data obtained at 1000 rpm. The rotating speed of the spindle may change in the actual machining process. For further verification of the proposed model, the experiments were carried out using various rotating speeds. The stepped spindle speed is presented in Fig. 10.

Since the contrast with and without compensation cannot be obtained using a single test, two tests were needed. As a result, one test was performed by using compensation and another without. The results with and without compensation are presented in Fig. 11.

Table 1 The residual errors of the two models

Rotating speed (rpm)	Range of residuals of model I (μm)	Range of residuals of model II (μm)
500	−2.76–0.77	−1.52–1.62
1000	−1.23–1.34	−1.26–5.05
1500	0–1.92	−1.23–3.39
2000	−1.86–2.78	−5.59–4.80

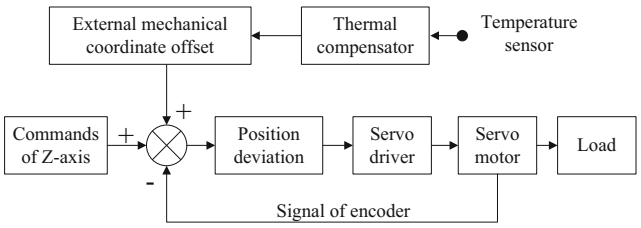

Fig. 9 Illustrative diagram of the compensation

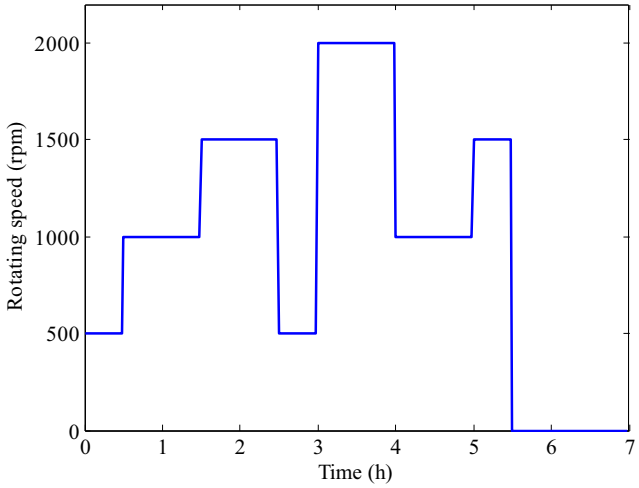

Fig. 10 Stepped spindle speed

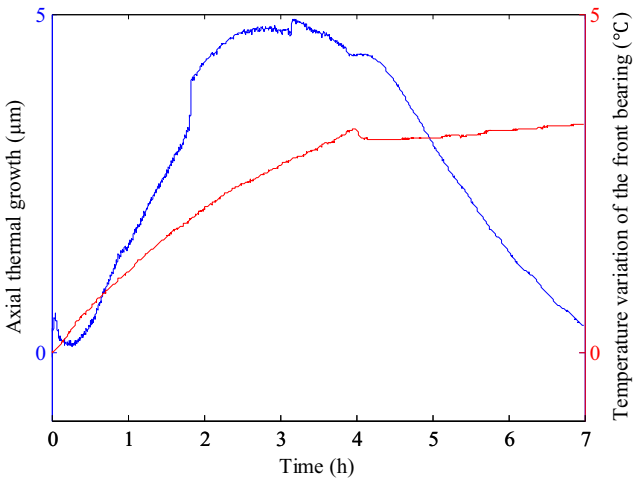

Fig. 12 Testing results at 500 rpm

It can be observed from Fig. 11 that the thermal growth error without compensation was fluctuating with the rotating speed of the spindle. The thermal growth error reached a maximum value of 13.7 μm at 2000 rpm. On the contrary, the range of residual error was between −2.2 and +1.5 μm, which was reduced to 16.1 % of the thermal growth error without compensation. It is clear that the predicted accuracy and robustness of the proposed model are good, even if the rotating speed of spindle changes randomly.

4.3.3 Further verification

The thermal growth of a spindle was tested on another kind of CNC turning machine at 500 rpm for further verification, using the same spindle error analyzer and temperature sensor as in Section 3.1. In these tests, the spindle was rotating at 500 rpm for 4 h and then remains stationary for 3 h. The tested results are presented in Fig. 12.

The parameters in the model were identified based on the data collected at 500 rpm of Fig. 12. Experimental verification was also carried out using various rotating speeds. The results with and without compensation are presented in Fig. 13.

It can be observed from Fig. 13 that the thermal growth error without compensation was fluctuating in the range of −0.96 to +10.91. On the contrary, the thermal growth error with compensation was fluctuating in the range of 0 to +2.65, even if the rotating speed of spindle was changing randomly.

5 Conclusions

A new axial thermal growth model for spindles, based on temperature variation, was proposed, and the principle of the model and the identification process of the parameters were

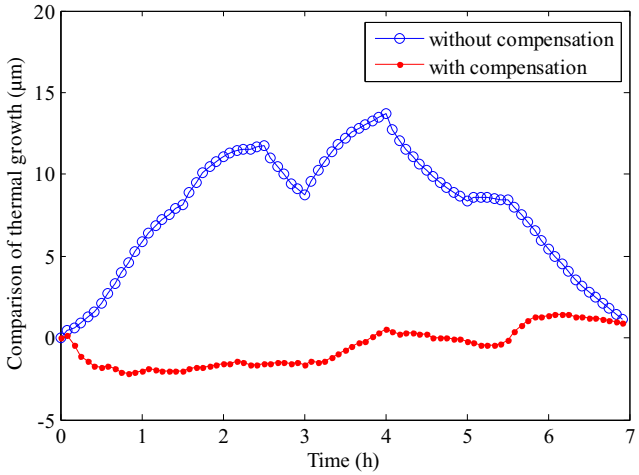

Fig. 11 Thermal growth errors with or without compensation

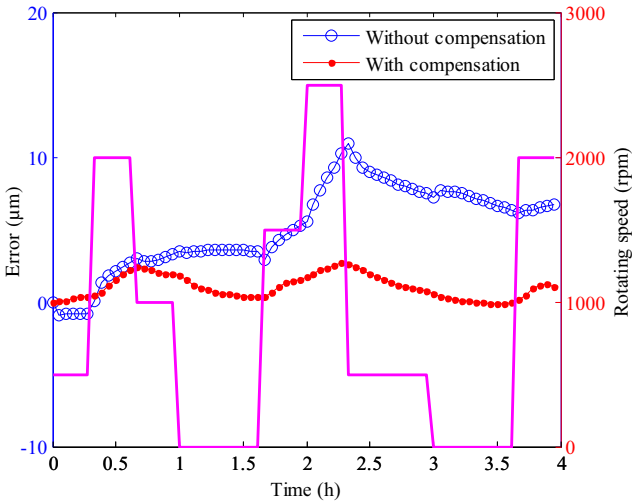

Fig. 13 Thermal growth errors with or without compensation

presented. The results collected by two turning machines show that the predicted accuracy and robustness of the proposed model were good, even when the rotating speed of the spindle was changing randomly. The proposed model is cost-effective, as it only needs one temperature sensor to function. Moreover, the tests for modeling may approximately last for 5–7 h, which makes it suitable for engineering applications.

Acknowledgments The authors gratefully acknowledge the support of "High-Grade CNC Machine Tool and Basic Manufacturing Equipment" Science and Technology Major Project (2013ZX04011011). Moreover, the authors would like to thank all the anonymous referees and editor for their valuable comments and suggestions.

References

1. Ramesh R, Mannan MA, Poo AN (2000) Error compensation in machine tools—a review. Part II: thermal errors. Int J Mach Tools Manuf 40(9):1257–1284
2. Yang J, Shi H, Feng B, Zhao L, Ma C, Mei XS (2015) Thermal error modeling and compensation for a high-speed motorized spindle. Int J Adv Manuf Tech 77(5-8):1005–1017
3. Mori M, Mizuguchi H, Fujishima M, Ido Y, Mingkai N, Konishi K (2009) Design optimization and development of CNC lathe headstock to minimize thermal deformation. CIRP Ann–Manuf Technol 58:331–334
4. Jiao Y, Sun LJ, Hong HB, Yin YH (2015) Material thermal conductivity determination and structure optimization of ultra-precision optical machine tool. J Mech Eng 51(1):167–175
5. Sun ZC, Tao T, Huang XY, Mei XS, Wang XM, Yang J, Zhao L (2015) Modeling and compensation of coupled thermal error of spindle and feed shafts. J Xi'an Jiaotong Univ 49(7):105–111
6. Mayr J, Jedrzejewwski J, Uhlmann E, Donmez MA, Knapp W, Hartig F, Wendt K, Moriwaki T, Shore P, Schmitt R, Brecher C, Wurz T, Wegener K (2012) Thermal issues in machine tools. CIRP Ann—Manuf Technol 61(2):771–791
7. Li Y, Zhao WH, Lan SH, Ni J, Wu WW, Lu BH (2015) A review on spindle thermal error compensation in machine tools. Int J Mach Tools Manuf 95:20–38
8. Lei CL, Rui ZY (2012) Thermal error modeling and forecasting based on multivariate autoregressive model for motorized spindle. Mech Sci Technol Aerosp Eng 31(9):1526–1529
9. Chen JS, Hsu WY (2003) Characterizations and models for the thermal growth of a motorized high speed spindle. Int J Mach Tools Manuf 43:1163–1170
10. Lin Z, Chang J (2007) The building of spindle thermal displacement model of high speed machine center. Int J Adv Manuf Tech 34:556–566
11. Wu CW, Tang CH, Chang CF, Shiao YS (2011) Thermal error compensation method for machine center. Int J Adv Manuf Tech 59:681–689
12. Krulewich DA (1998) Temperature integration model and measurement point selection for thermally induced machine tool errors. Mechatronics 8:395–412
13. Yang H, Ni J (2005) Dynamic neural network modeling for nonlinear, nonstationary machine tool thermally induced error. Int J Mach Tools Manuf 45:455–465
14. Zhang Y, Yang JG, Jiang H (2012) Machine tool thermal error modeling and prediction by grey neural network. Int J Adv Manuf Tech 59:1065–1072
15. Xiang ST, Yang JG, Zhang Y (2014) Modeling method for spindle thermal error based on mechanism analysis and thermal basic characteristics tests. J Mech Eng 50(11):144–152
16. Yang JG, Fan KG (2013) Research on the thermal deformation pseudo-lag and real-time compensation for CNC machine tool spindle. J Mech Eng 49(23):129–135
17. Yang J (1999) Thermal error mode analysis and robust modeling for error compensation on a CNC turning center. Int J Mach Tools Manuf 39:1367–1381
18. Zhu J (2008) Robust thermal error modeling and compensation for CNC machine tools. Dissertation, University of Michigan
19. Shu QL, Li YL, Lv YS (2012) Application of time series analysis to thermal error modeling on NC micro-grinder. Mod Mach Tool Auto Manuf Tech 12:30–32
20. Li YX, Tong HC, Cao HT, Zhang HT, Yang JG (2006) Application of time series analysis to thermal error modeling on NC machine tool. J Sichuan Univ (Eng Sci Ed) 38(2):74–78
21. Lin WQ, Fu JZ, Chen ZC, Xu YZ (2009) Modeling of NC machine tool thermal error based on adaptive best-fitting WLS-SVM. J Mech Eng 45(3):178–182
22. Xu Y Z (2006) Research on thermal error modeling of machine tools based on least squares support vector machine. Dissertation, Zhejiang University
23. Miao EM, Gong YY, Xu ZS, Zhou XS (2015) Comparative analysis of thermal error compensation model robustness of CNC machine tools. J Mech Eng 51(7):130–135
24. Jiang H, Yang JG, Yao XD, Zhang YS, Yuan F (2013) Modeling of CNC machine tool spindle thermal distortion with LS-SVM based on Bayesian inference. J Mech Eng 49(15):115–121
25. Creighton E, Honegger A, Tulsian A, Mukhopadhyay D (2010) Analysis of thermal errors in a high-speed micro-milling spindle. Int J Mach Tools Manuf 50:386–393
26. ISO 230-2: 2006 (2006) Test code for machine tools—part 2: determination of accuracy and repeatability of positioning numerically controlled axes. International Standards Organization, Switzerland